

# Oxidation kinetics of low-oxygen silicon carbide fiber

T. SHIMOO

*Department of Metallurgy and Materials Science, College of Engineering,  
Osaka Prefecture University, 1-1, Gakuen-cho, Sakai, Osaka 599-8531, Japan*

F. TOYODA

*Osaka Prefecture University, 1-1, Gakuen-cho, Sakai-shi, Osaka 599-8531, Japan*

K. OKAMURA

*Department of Metallurgy and Materials Science, College of Engineering,  
Osaka Prefecture University, 1-1, Gakuen-cho, Sakai, Osaka 599-8531, Japan*

---

The effect of partial pressure and temperature on the oxidation rate of low-oxygen silicon carbide fiber (Hi-Nicalon) has been investigated. The initial oxidation rate was described by a two-dimensional disc contracting formula for reaction control, and the activation energy was 155 kJ/mol. The rate at the later stage of oxidation obeyed the equation for diffusion control, and the activation energy was 109 kJ/mol. Both the rate constants were proportional to oxygen partial pressure. The diffusion species through the SiO<sub>2</sub> film are considered to be oxygen molecules. © 2000 Kluwer Academic Publishers

---

## 1. Introduction

Low-oxygen silicon carbide fiber, fabricated from polycarbosilane by an electron beam-curing method (Trade name: Hi-Nicalon, Nippon Carbon Co.), has a nano-scale micro-structure which is composed of  $\beta$ -SiC crystallites, free carbon and amorphous oxycarbide, SiC<sub>x</sub>O<sub>y</sub> [1]. When the fiber is exposed to elevated temperatures, the SiC<sub>x</sub>O<sub>y</sub> phase crystallizes into  $\beta$ -SiC, with the generation of both SiO and CO gases. Since such a high-temperature decomposition reaction results in the coarsening of SiC crystals and serious damage to the fiber structure by gas generation, considerable degradation of fiber strength occurs [2–7]. Compared with silicon carbide fibers fabricated by the oxidation-curing method (Trade name: Nicalon, Nippon Carbon Co.), the high-temperature characteristics of Hi-Nicalon were greatly improved by reducing the oxygen content.

In addition to the reduction of oxygen content, the oxidation treatment was also found to be effective for suppressing the high-temperature decomposition of the silicon carbide fiber [8, 9]. This is because the SiO<sub>2</sub> film formed on fiber surface disturbed the escape of decomposition gases evolved, SiO and CO. Therefore, the oxidation treatment is thought to be efficient in improving further the thermal stability of Hi-Nicalon. Since the controlling factors such as thickness, density, crystallinity and adherence of the SiO<sub>2</sub> film have a great influence on the suppression of decomposition of the fiber core, it is necessary to study the growth mechanism of SiO<sub>2</sub> film. The change in reaction mechanism during oxidation and the different diffusion species in the SiO<sub>2</sub> film, O<sub>2</sub> molecule and O<sup>2-</sup> ion, were observed for SiC powder and SiC ceramics [10–16]. However, from

such a standpoint, research on the oxidation of Nicalon and Hi-Nicalon has not been performed [17–22]. In a previous report, the authors investigated the effect of oxygen partial pressure and temperature on the oxidation rate of Nicalon in order to elucidate the diffusion species in the SiO<sub>2</sub> film, the reaction mechanism and the rate-determining step [23]. In the present study, the oxidation of Hi-Nicalon was studied in detail and its reaction mechanism was compared with those of Nicalon, SiC powder and SiC ceramics.

## 2. Experimental procedure

The silicon carbide fiber used in the present work is a polycarbosilane-derived low-oxygen fiber (Hi-Nicalon produced in the form of yarn with about 500 fibers per tow by Nippon Carbon Co. Ltd.). It has the composition of SiC<sub>1.40</sub>O<sub>0.05</sub> and mean diameter of 15  $\mu$ m. The thermobalance unit used for the measurement of oxidation rate is composed of an auto-recording balance (sensitivity: 0.1 mg) and a silicon carbide resistance furnace.

Fibers, 1 g in mass and 1 cm in length, were contained in a magnesia crucible of 26 mm inner diameter and 50 mm in depth. The magnesia crucible was previously heated in air at 1773 K until the ignition loss was not observed. The magnesia crucible was suspended in the hot zone of the furnace with a platinum wire which was connected to the balance. A dry Ar-O<sub>2</sub> gas mixture was allowed to flow from the bottom of the furnace at a flow rate of 500 cm<sup>3</sup>/min. At 1573 K, the oxidation rates were measured under oxygen pressures of 0.25, 0.5, 0.75 and 1 atm. Then, under oxygen partial pressure of 0.25 atm, they were measured at temperatures

from 1473 to 1773 K. The mass gain was recorded automatically during each experiment. Upon completion of a thermogravimetric measurement, the fibers were quenched by raising the crucible to the low-temperature zone of the furnace. The rate data obtained by thermogravimetric measurements were submitted to kinetic analysis in order to clarify the oxidation mechanism of Hi-Nicalon.

### 3. Results and discussion

Figs 1 and 2 show the TG curves for fibers oxidized under different partial pressures of oxygen and at different temperatures, respectively.  $W_0$  and  $\Delta W$  are the initial mass of fibers and the mass gain measured by the thermobalance, respectively. Oxidation of Hi-Nicalon

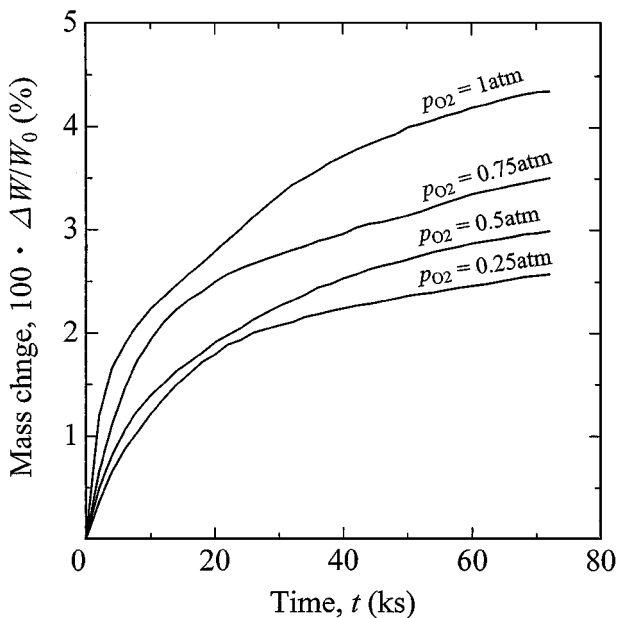


Figure 1 TG curves for Hi-Nicalon heated in different Ar-O<sub>2</sub> gas mixtures at 1573 K.

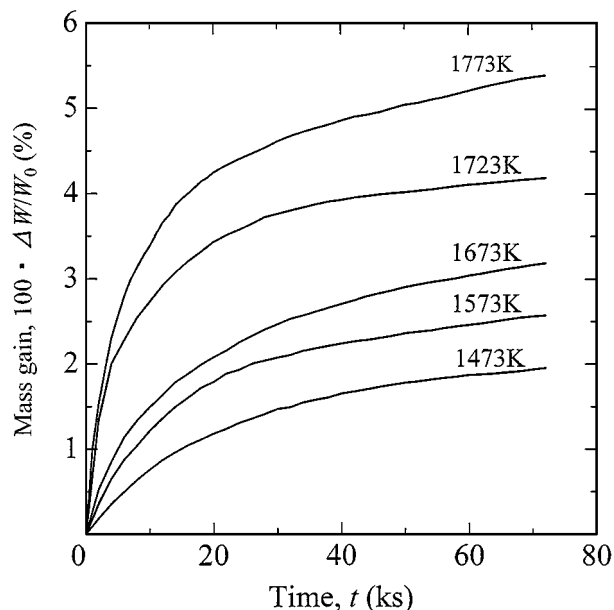


Figure 2 TG curves for Hi-Nicalon heated in Ar-25% O<sub>2</sub> gas mixture at different temperatures.

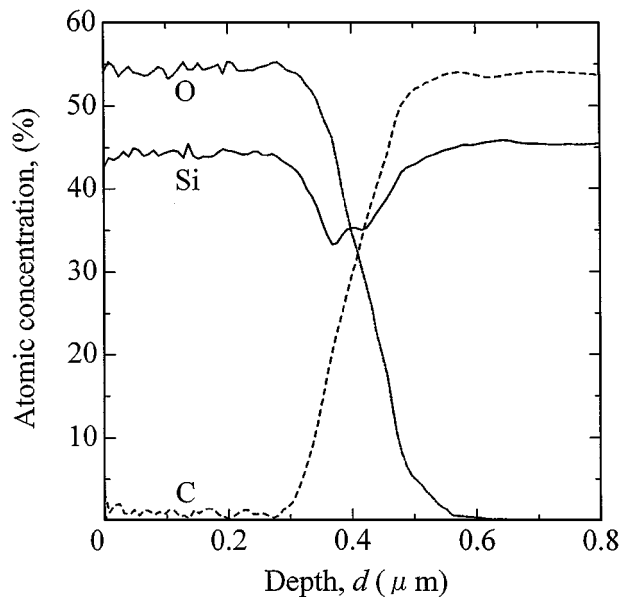


Figure 3 AES depth profile of fiber heated for 72 ks in Ar-25% O<sub>2</sub> gas mixture at 1573 K.

resulted in a mass gain which was accelerated by increasing oxygen partial pressure and temperature. The mass gain is due to the following overall reaction:

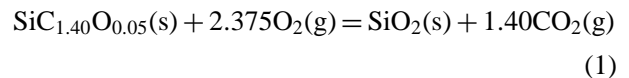


Fig. 3 shows the Auger electron spectroscopic measurement of the surface composition for a fiber oxidized for 72 ks in an Ar-25% O<sub>2</sub> gas mixture at 1573 K. An SiO<sub>2</sub> film of about 0.3 μm is formed on the fiber core. The formation of an SiO<sub>2</sub> film was also confirmed by scanning electron microscopic observation. Therefore, the SiO<sub>2</sub> film grows during oxidation and the reaction interface recedes towards the center of fiber as the oxidation progresses.

The oxidation of Hi-Nicalon fiber proceeds through the following basic steps:

- (1) Diffusion of oxygen from the gas phase to the SiO<sub>2</sub> film surface through the space between fibers
- (2) Diffusion of oxygen through the SiO<sub>2</sub> film
- (3) Chemical reaction at the interface between the SiO<sub>2</sub> film and the unoxidized core
- (4) Diffusion of CO<sub>2</sub> through the SiO<sub>2</sub> film
- (5) Diffusion of CO<sub>2</sub> to the gas phase through the space between fibers

These five steps may be regrouped as follows:

- (1) Gaseous diffusion through the space between fibers
- (2) Diffusion through the SiO<sub>2</sub> film
- (3) Chemical reaction at the interface

The overall rate equations, in which both reaction kinetics and oxygen diffusion were taken into account, were proposed: the linear-parabolic rate law for the oxidation of silicon plate and the contracting disc model for that of Nicalon fiber [22, 24]. However, the application

of the overall rate equations to kinetic data are very much complicated. In present work, for simplicity, the kinetic data were separately applied to the rate equation for each step of the oxidation of SiC fiber.

Gaseous diffusion is not considered to be the rate-determining step because of large diffusivity. In addition, at the earliest stage of oxidation, the resistance of the diffusion through the SiO<sub>2</sub> film to the oxidation rate is relatively small because of thin SiO<sub>2</sub> film. Therefore, the initial rate may be controlled solely by the chemical reaction at the interface (step (3)). Oxidation can take place only at the reaction interface and therefore the oxidation rate should be proportional to the interface area. If the oxidation of fibers is controlled by an irreversible first-order reaction at the interface between the SiO<sub>2</sub> film and the unoxidized core, the oxidation rate,  $n$ , can be expressed by the following equation:

$$n = 2\pi r_1 L k_r C^* \quad (2)$$

where  $r_1$ : the radius of unoxidized core (m),  $L$ : the length of fiber (m),  $k_r$ : the rate constant for forward reaction (m/s),  $C^*$ : the oxygen concentration at the surface of fiber (mol/m<sup>3</sup>).

The oxidation rate also can be described by the equation:

$$\begin{aligned} n &= \frac{d\{(\pi r_0^2 L - \pi r_1^2 L)d_0\}}{dt} \\ &= -2\pi r_1 L d_0 \left( \frac{dr_1}{dt} \right) \end{aligned} \quad (3)$$

where  $r_0$  is the initial radius of the fiber (=7.5 μm) and  $d_0$  is the density of oxygen in the SiO<sub>2</sub> film (mol/m<sup>3</sup>). In addition, the oxidized fraction of fibers,  $X$  is defined as follows:

$$X = 1 - \left( \frac{r_1}{r_0} \right)^2 \quad (4)$$

From the stoichiometry of reaction (1), the oxidized fraction,  $X$ , of Hi-Nicalon is given by:

$$X = \frac{3.167 \times \Delta W}{W_0} \quad (5)$$

where  $\Delta W$  is the mass gain of the fiber during oxidation and  $W_0$  is the initial mass of the fibers. Combining Equations 2–4 yields the following two-dimensional disc-contracting rate equation for reaction control:

$$1 - (1 - X)^{1/2} = k_r t \quad (6)$$

$$k_r = \frac{k'_r C^*}{r_0 d_0} \quad (7)$$

where  $k_r$  is the rate constant for chemical reaction (step (3)).

As a consequence of thickening of the SiO<sub>2</sub> film during oxidation, the rate-determining step changes to diffusion through the SiO<sub>2</sub> film (step (2)). Thus, the oxidation rate at the later stage obeys Fick's first law of diffusion:

$$n = 2\pi r L D_0 \left( \frac{dC}{dt} \right) \quad (8)$$

where  $D_0$  is the diffusion coefficient of oxygen in the SiO<sub>2</sub> film. Integrating Equation 8 and combining with Equations 3 and 4 gives the following two-dimensional disc-contracting rate equation for diffusion control:

$$(1 - X) \ln(1 - X) + X = k_d t \quad (9)$$

$$k_d = \frac{D_0 C^*}{r_0 d_0} \quad (10)$$

where  $k_d$  is the rate constant for step (2). In addition, the oxygen concentration at the interface between the SiO<sub>2</sub> film and the unoxidized core is negligibly small.

Oxygen diffuses in the SiO<sub>2</sub> film as either ions (O<sup>2-</sup>) or molecules (O<sub>2</sub>). Oxygen gas, therefore, dissolves in the SiO<sub>2</sub> film as dissociated ions or molecules. The dissolution reactions and equilibrium constants can be represented as follows:

$$\begin{aligned} \text{O}_2(\text{g}) &= 2\text{O}^{2-} \text{ (in SiO}_2 \text{ film)} \\ K_{\text{O}} &= \frac{C^{*2}}{p_{\text{O}_2}} \end{aligned} \quad (11)$$

$$\begin{aligned} \text{O}_2(\text{g}) &= \text{O}_2 \text{ (in SiO}_2 \text{ film)} \\ K_{\text{O}_2} &= \frac{C^*}{p_{\text{O}_2}} \end{aligned} \quad (12)$$

The solubility of oxygen in SiO<sub>2</sub>,  $C^*$ , is proportional to  $p_{\text{O}_2}^{1/2}$  for ions and  $p_{\text{O}_2}$  for molecules, respectively. Consequently, the rate constants are also proportional to either  $p_{\text{O}_2}^{1/2}$  or  $p_{\text{O}_2}$ , as described below.

For oxygen ions:

$$k_r = \frac{k'_r K_{\text{O}}^{1/2} p_{\text{O}_2}^{1/2}}{r_0 d_0} \quad (13)$$

$$k_d = \frac{D_0 K_{\text{O}}^{1/2} p_{\text{O}_2}^{1/2}}{r_0 d_0} \quad (14)$$

For oxygen molecules:

$$k_r = \frac{k'_r K_{\text{O}_2} p_{\text{O}_2}}{r_0 d_0} \quad (15)$$

$$k_d = \frac{D_0 K_{\text{O}_2} p_{\text{O}_2}}{r_0 d_0} \quad (16)$$

Figs 4 and 5 show the application of the rate Equations 6 and 9 to the TG data, respectively. For the reaction control regime, the plots of  $1 - (1 - X)^{1/2}$  vs.  $t$  gave a linear relationship at the earliest stage of oxidation (within 3 ks), which the oxidized fraction,  $X$ , is smaller than about 0.015. The thickness of the SiO<sub>2</sub> film,  $b$ , can be estimated by the following equation:

$$b = r_0 \times \{1 - (1 - X)^{1/2}\} \quad (17)$$

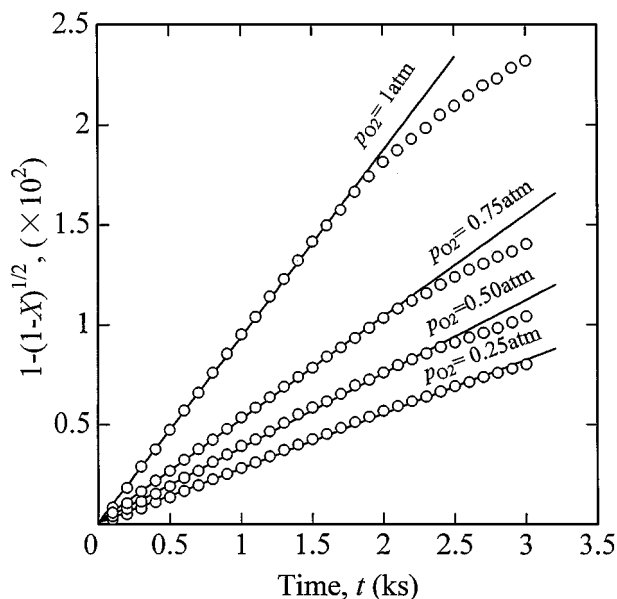


Figure 4 Application of two-dimensional contracting-disc formula for reaction control to rate data shown in Fig. 1.

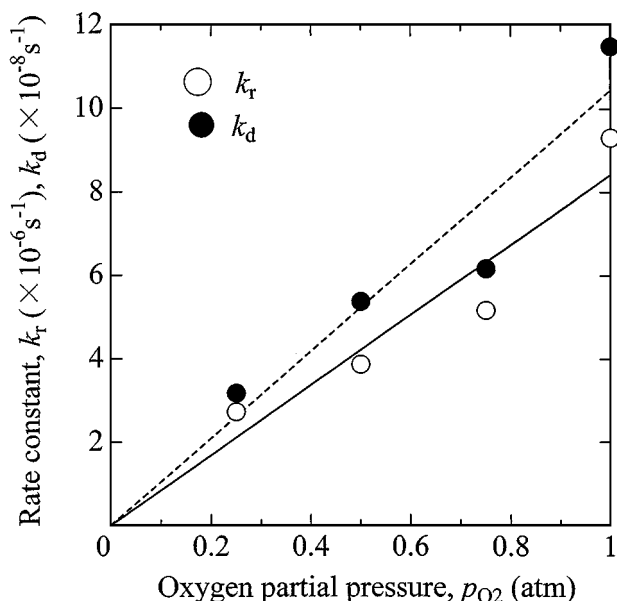


Figure 6 Relationship between rate constants and oxygen partial pressure.

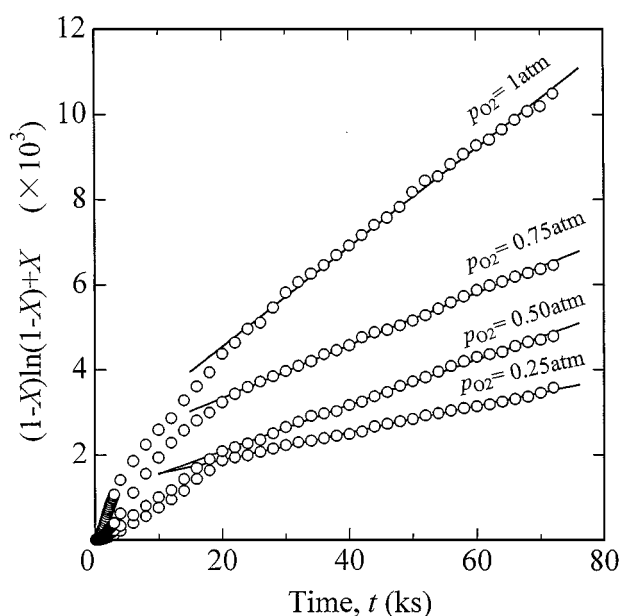


Figure 5 Application of two-dimensional contracting-disc formula for diffusion control to rate data shown in Fig. 1.

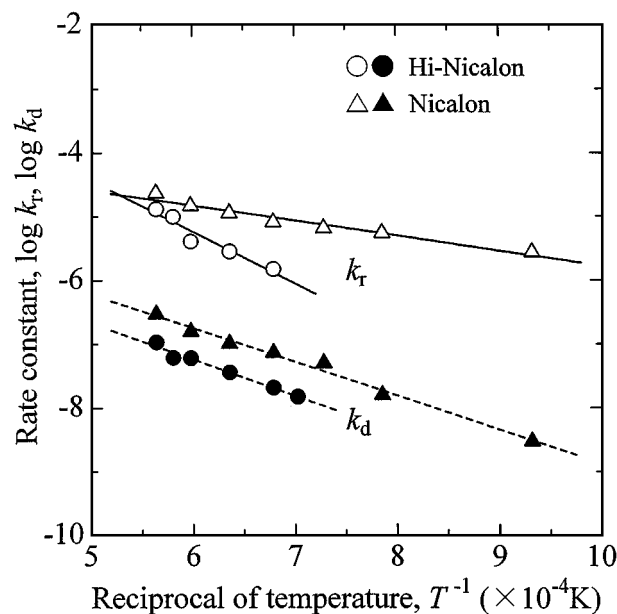


Figure 7 Arrhenius plots for rate constants.

where,  $r_0$  is  $7.5 \mu\text{m}$ . The above oxidized fraction of 0.015, therefore, corresponds to the film thickness of  $5.6 \times 10^{-2} \mu\text{m}$ . Thus, the rate Equation 6 is applicable to the rate data only for very thin  $\text{SiO}_2$  films. When the  $\text{SiO}_2$  film grew sufficiently and the rate-determining step changed to the diffusion through the  $\text{SiO}_2$  film, the linear dependence between  $(1-X)\ln(1-X)+X$  and  $t$  was found to hold. The rate constants are obtained from the slopes of each straight line. The linear dependence of the rate constants,  $k_r$  and  $k_d$ , on  $p_{\text{O}_2}^{1/2}$  could not be found at all. On the other hand, as can be seen from Fig. 6, the plots of rate constants against  $p_{\text{O}_2}$  reveals approximately linear relationships. Thus, the relationship between the rate constants,  $k_r$  and  $k_d$ , and oxygen partial pressure satisfied Equations 15 and 16, respectively. Therefore, oxygen molecules dissolve

and diffuse in the  $\text{SiO}_2$  film of Hi-Nicalon, as well as in that of Nicalon [23].

The logarithm of rate constants,  $k_r$  and  $k_d$ , are plotted against the reciprocal of absolute temperature in Fig. 7. It may be noted that the rate constants for Hi-Nicalon are smaller than those for Nicalon. This result is thought to be related to different microstructure: small size of  $\beta$ -SiC crystals (1–4 nm), large amounts of amorphous  $\text{SiC}_x\text{O}_y$  phase and small amounts of free carbon for Nicalon and relatively large size of  $\beta$ -SiC crystals (2–20 nm), very small amounts of amorphous  $\text{SiC}_x\text{O}_y$  phase and large amounts of free carbon for Hi-Nicalon [1, 20, 21, 25–28]. However, further investigation is required to give a full account of this result. The plots reveal an approximately linear relationship. From the Arrhenius equation, the activation energies for both interfacial reaction control and diffusion control

through the SiO<sub>2</sub> film,  $E_r$  and  $E_d$ , can be evaluated to be 155 kJ/mol and 109 kJ/mol, respectively. The rate constants for Nicalon are also shown in Fig. 7 and the resulting activation energies,  $E_r$  and  $E_d$ , were 45 kJ/mol and 102 kJ/mol, respectively [23].

The value  $E_r$  (155 kJ/mol) for Hi-Nicalon is much larger than observed for Nicalon (45 kJ/mol). The high level of  $E_r$  for the oxidation of Hi-Nicalon is reasonable as the activation energy of interfacial reaction. On the other hand, the low level of  $E_r$  implies that the oxidation of Nicalon is not controlled only by the interfacial reaction. The diffusion coefficient of gases increases with the 1.5–1.8 power of the absolute temperature [29]. From such a temperature dependence, the activation energy for the gaseous diffusion is estimated to be 17–20 kJ/mol at the experimental temperature range from 1073 to 1773 K. Therefore, the contribution of step (1) (gaseous diffusion through the space between fibers) to the initial oxidation rate seems to be responsible for the low value of  $E_r$ . Compared to the activation energy of gaseous diffusion, however, the value  $k_r$  of 45 kJ/mol is greater by a factor of 2–3. This indicates that the initial oxidation rate of Nicalon is thought to be controlled by both the gas-phase diffusion and interfacial reaction. Since the rapid oxidation will cause the insufficient supply of O<sub>2</sub> gas to the unoxidized surface, the resistance of gaseous diffusion to the oxidation rate of Nicalon is large and the value  $E_r$  is consequently low. On the other hand, Hi-Nicalon which has slow oxidation rate is principally controlled by the interfacial reaction and has a high level of  $E_r$ . With increasing temperature, the oxidation rate of Hi-Nicalon approaches that of Nicalon. Therefore, the resistance of gaseous diffusion to the oxidation rate of Hi-Nicalon is not negligible at elevated temperature.

Table I shows the kinetic parameters for the diffusion-controlled oxidation of SiC powder, SiC ceramics and SiC fiber [10–21, 23]. For the oxidation of SiC powder and SiC ceramics, the diffusion of oxygen ions in the SiO<sub>2</sub> film were verified by the dependence of  $k_d$  on  $p_{O_2}^{1/2}$  and high activation energies (190–498 kJ/mol). On the other hand, the diffusion of O<sub>2</sub> molecules gave low activation energies (65–155 kJ/mol). The different diffusion species are thought to be due to the oxygen permeability of the SiO<sub>2</sub> film formed around SiC ceramics.

In present work, the low activation energies ( $E_d = 109$  kJ/mol) was obtained for the oxidation of Hi-Nicalon in Ar-O<sub>2</sub> gas mixture ( $p_{O_2} = 0.25$  atm), being almost identical to that for Nicalon ( $E_d = 102$  kJ/mol) [23]. Chollon *et al.* also obtained the low activation energies of 69–96 kJ/mol for the oxidation of Nicalon and Hi-Nicalon in flowing pure oxygen [20, 21]. On the other hand, the author obtained rather high activation energies in flowing pure oxygen: 137 kJ/mol for Nicalon and 234 kJ/mol for Hi-Nicalon [19]. The activation energy of Hi-Nicalon, however, was estimated to be 162 kJ/mol for the same temperature range as present work (1473–1773 K). According to author's studies, the activation energies for the oxidation under one atmospheric pressure of oxygen were greater than those for the oxidation under Ar-O<sub>2</sub> gas mixture with oxygen partial pressure of 0.25. However, the reason why higher oxygen partial pressure caused an increase of activation energy is unknown. The dependence of  $k_d$  on  $p_{O_2}$  and low activation energies show that the oxidation rates are controlled by the diffusion of O<sub>2</sub> molecules through the SiO<sub>2</sub> film formed around SiC fibers. Since both Nicalon and Hi-Nicalon fibers have a number of microvoids, O<sub>2</sub> molecules are thought to

TABLE I Kinetic parameters for diffusion-controlled oxidation of SiC

Sample	Dependence of $k_d$ on $p_{O_2}$	Activation Energy	Diffusing species	Reference
SiC powder		85 kJ/mol	O <sub>2</sub> molecule (amorphous silica)	Jorgensen [10]
SiC powder	$p_{O_2}^{1/2}$ no	65 kJ/mol	O <sub>2</sub> molecule (cristobalite)	Jorgensen [11]
		190 kJ/mol	oxygen ion	
			CO molecule	Pultz [12]
			O <sub>2</sub> molecule (1273–1673 K) CO molecule (1673–1873 K)	Fitzer [13]
Hot pressed SiC		155 kJ/mol	O <sub>2</sub> molecule (below 1673 K)	Costello [14]
$\alpha$ -SiC ceramics	$p_{O_2}^{1/2}$	498 kJ/mol	oxygen ion (above 1673 K)	Costello [15]
		134 kJ/mol	O <sub>2</sub> molecule (below 1673 K)	
CVD SiC	$p_{O_2}^{1/2}$	389 kJ/mol	oxygen ion (above 1673 K)	Narushima [16]
		345 kJ/mol	oxygen ion (amorphous silica)	
Nicalon	$p_{O_2}^{1/2}$	387 kJ/mol	oxygen ion (cristobalite)	Filipuzzi [17]
pure O <sub>2</sub> gas		69–77 kJ/mol		Shimoo [19]
pure O <sub>2</sub> gas		137 kJ/mol		Chollon [20]
pure O <sub>2</sub> gas		107 kJ/mol		Chollon [21]
pure O <sub>2</sub> gas		90 kJ/mol		Chollon [21]
Ar-O <sub>2</sub> gas mixture	$p_{O_2}$	102 kJ/mol	O <sub>2</sub> molecule	Shimoo [23]
Hi-Nicalon				
pure O <sub>2</sub> gas		162 kJ/mol <sup>a</sup>		Shimoo [19]
pure O <sub>2</sub> gas		107 kJ/mol		Chollon [20]
pure O <sub>2</sub> gas		96 kJ/mol		Chollon [21]
Ar-O <sub>2</sub> gas mixture	$p_{O_2}$	109 kJ/mol	O <sub>2</sub> molecule	Present work

<sup>a</sup>Estimated in the temperature range from 1473 to 1773 K.

be permeable into the SiO<sub>2</sub> films formed around the fibers [30, 31].

#### 4. Conclusion

Low-oxygen content silicon carbide fiber (Hi-Nicalon) was oxidized under oxygen partial pressures from 0.25 to 1 atm at temperatures from 1473 to 1773 K. The oxidation mechanism of Hi-Nicalon was proposed by carrying out the kinetic analysis of TG data.

In the earliest stage of oxidation, Hi-Nicalon obeyed the two-dimensional disc-contracting rate equation for reaction control. The rate constants,  $k_r$ , was proportional to the partial pressure of oxygen gas,  $p_{O_2}$ . The apparent activation energy for chemical reaction was estimated to be 155 kJ/mol. The initial rate is determined by chemical reaction between O<sub>2</sub> gas and unoxidized core.

The oxidation rate at later stages was described by the two-dimensional disc-contracting rate equation for diffusion control. The proportionality between the rate constant,  $k_d$ , and  $p_{O_2}$  was found to hold. The apparent activation energy was 109 kJ/mol.

It is thought that oxygen molecules diffuse through the SiO<sub>2</sub> film to oxidize Hi-Nicalon at the interface between the SiO<sub>2</sub> film and the unoxidized core.

#### Acknowledgement

This study was supported in part by the Ministry of Education, Science, Sports and Culture under Grant No. 11450255.

#### References

1. C. LAFFON, A. M. FLANK, P. LAGARDE, M. LARIDJANI, R. HAGEGE, P. OLRV, J. COTTERET, J. DIXMIER, J. L. MIQUEL, H. HOMMEL and A. P. LAGRAND, *J. Mater. Sci.* **24** (1989) 1503.
2. M. JOHNSON, R. D. BRITAIN, R. H. LAMOREAUX and D. J. ROWCLIFF, *J. Amer. Ceram. Soc.* **71** (1988) C-132.
3. T. SHIMOO, M. SUGIMOTO and K. OKAMURA, *J. Japan Inst. Metals* **54** (1990) 802.
4. E. BOUILLON, F. LANGLAIS, R. PAILLER, R. NASLAIN, P. V. HUONG, J. C. SARTHOU, A. DELPUECH, C. LAFFON, P. LAGARDE, M. MONTHIOUX and A. OBERLIN, *J. Mater. Sci.* **26** (1991) 1333.
5. T. SHIMOO, H. CHEN and K. OKAMURA, *J. Ceram. Soc. Jpn.* **100** (1992) 48.
6. C. VAHLAS, P. ROCABOIS and C. BERNARD, *J. Mater. Sci.* **29** (1994) 5839.
7. *Idem.*, *ibid.* **30** (1995) 1558.
8. T. SHIMOO, H. CHEN, K. KAKIMOTO and K. OKAMURA, *J. Ceram. Soc. Jpn.* **101** (1993) 295.
9. T. SHIMOO, H. CHEN and K. OKAMURA, *J. Japan Inst. Metals* **57** (1993) 652.
10. P. J. JORGENSEN, M. E. WADSWORTH and I. B. CUTLER, *J. Amer. Ceram. Soc.* **42** (1959) 613.
11. *Idem.*, *ibid.* **43** (1960) 209.
12. W. W. PULTZ, *J. Phys. Chem.* **71** (1967) 4556.
13. F. FITZER and R. EBI, "Silicon Carbide" (University of South Carolina Press, Columbia, 1974) p. 320.
14. J. A. COSTELLO and R. E. TRESSLER, *J. Amer. Ceram. Soc.* **64** (1981) 327.
15. *Idem.*, *ibid.* **69** (1986) 674.
16. T. NARUSHIMA, T. GOTO and T. HIRAI, *ibid.* **72** (1989) 1386.
17. L. FILIPUZZI and R. NASLAIN, in Proceedings of 7th CIMTEC, Satellite Symposium 2 (S2.1-L03), Montecatini, Terme-Italy, June 1990, p. 35.
18. T. SHIMOO, H. CHEN and K. OKAMURA, *J. Ceram. Soc. Jpn.* **100** (1992) 929.
19. T. SHIMOO, T. HAYATSU, M. TAKEDA, H. ICHIKAWA, T. SEGUCHI and K. OKAMURA, *ibid.* **102** (1994) 617.
20. G. CHOLLON, R. R. PAILLER, R. NASLAIN, F. LAANANI, M. MONTHIOUX and P. OLRV, *J. Mater. Sci.* **32** (1997) 327.
21. G. CHOLLON, M. CZERNIAK, R. PAILLER, X. BOURRAT, R. NASLAIN, J. P. PILLOT and R. CANNET, *ibid.* **32** (1997) 893.
22. Y. T. ZHU, S. T. TAYLOR, M. G. STOUT, D. P. BUTT and T. C. LOWE, *J. Amer. Ceram. Soc.* **81** (1998) 655.
23. T. SHIMOO, F. TOYODA and K. OKAMURA, *J. Ceram. Soc. Jpn.* **106** (1998) 447.
24. B. E. DEAL and A. S. GROVE, *J. Appl. Phys.* **36** (1965) 3770.
25. P. LECOUSTUMER, M. MONTHIOUX and A. OBERLIN, *J. Eur. Ceram. Soc.* **11** (1993) 95.
26. M. H. BERGER, N. HOCHET and A. R. BUNSELL, *J. Microscopy* **177** (1995) 230.
27. N. HOCHET, M. H. BERGER and A. R. BUNSELL, *ibid.* **185** (1997) 243.
28. G. CHOLLON, R. PAILLER, R. NASLAIN and P. OLRV, *J. Mater. Sci.* **32** (1997) 1133.
29. J. SZEKELY and N. J. THEMELIS, "Rate Phenomena in Process Metallurgy" (Wiley-Interscience Inc., New York, 1971) p. 368.
30. L. C. SAWYER, M. JAMIESON, D. BRIKOWSKI, M. I. HAIDER and R. T. CHEN, *J. Amer. Ceram. Soc.* **70** (1987) 798.
31. K. SUZUYA, M. FURUSAKA, N. WATANABE, M. OSAWA, K. OKAMURA, K. SHIBATA, T. KAMIYAMA and K. SUZUKI, *J. Mater. Res.* **11** (1996) 1169.

Received 25 May 1999  
and accepted 14 January 2000